Mendeleev Commun., 2027, **37**, just accepted

Mendeleev Communications

26/8170

Received 07.08.26
Revised 11.11.26

Silver wheel incorporating acetone oxalohydrazide dihydrazone: structure, thermal stability and luminescent properties

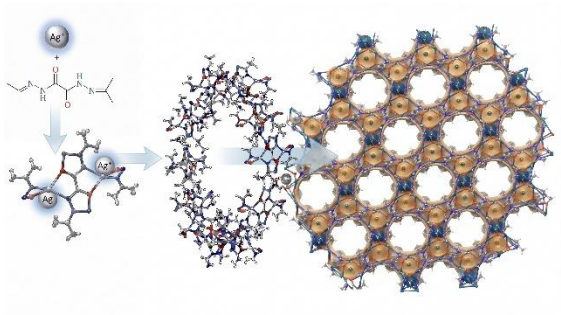
Kseniya A. Koshenskova,*[a] Fedor M. Dolgushin,[a] Leonid D. Popov,[b] Mikhail A. Kiskin,[a] Anton V. Gus`kov,[a] Igor L. Eremenko[a] and Irina A Lutsenko*[a]

[a] *N.S. Kurnakov Institute of General and Inorganic Chemistry, Russian Academy of Sciences, 119071 Moscow, Russian Federation. Fax: +7 495 952 1279; e-mail: ksenia-18.11.99@mail.ru; irinalu05@rambler.ru*

[b] *Southern Federal University, 344006 Rostov-on-Don, Russian Federation*

DOI: 10.71267/mencom.8170

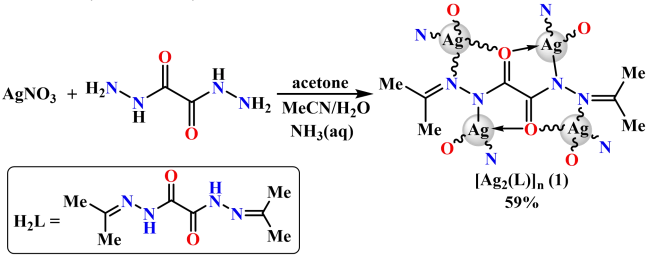
A new silver(I) coordination polymer $[Ag_2L]_n$ (1) (L^{2-} = dianion of acetone oxalohydrazide dihydrazone) was prepared by *in situ* condensation of oxalohydrazide with acetone and $AgNO_3$. In the crystal, it forms a 3D honeycomb-like channel framework (channel dimensions ~9.3 × 4.9 Å) assembled from non-equivalent five-membered N,O-chelate rings (one planar, one envelope), with L^{2-} coordinating all heteroatoms to Ag^+. Thermolysis is multistage and up to 500 °C gives silver nanoparticles, while the solid-state emission spectrum at λ_{ex} = 260 nm consists of broad bands with maxima at 427, 490 and 536 nm and is assigned to ligand-centered fluorescence.



Keywords: silver(I), coordination polymer, oxalohydrazide, crystal structure, thermal stability, luminescence.

Coordination compounds of silver(I) attract the attention of researchers due to the high flexibility of the Ag^+ cation, which is due to the electron configuration $[Kr]4d^{10}$ and the absence of stereochemical directionality. This allows it to bind both hard and soft donor atoms to form structures ranging from mononuclear to 3D coordination polymers and realize coordination numbers from 2 to 8.[1–6] The structural diversity and properties of silver(I) complexes are extremely sensitive to the ligand environment, the nature of counterions and solvents, and non-covalent interactions, making them promising candidates for catalytic, luminescent, and medical applications.[7–11] Among the wide variety of ligands, hydrazone-based Schiff bases represent versatile polydentate systems due to the presence of an azomethine group (–C=NNH–) and a carbonyl moiety (C=O), which allows them to coordinate in neutral or deprotonated forms through N,N- or N,O-donor atoms to form chelate, bridged, or polymeric structures.[12–14] In particular, derivatives oxalohydrazide, when condensed with ketones, forms tetradentate Schiff bases of the type $(R)_2C{=}NNH{-}CO{-}CO{-}NHN{=}C(R)_2$, capable of realizing both chelate and bridging coordination modes.[15] Analysis of the The Cambridge Structural Database (CSD version 5.45, November 2023) shows that silver(I) complexes with oxalohydrazide dihydrazone ligands remain relatively poorly studied in structural terms – there is only one structure with a ligand of this type $[Ag_2(\mu_2\text{-}H_2L)(PPh_3)_2(H_2O)_2](NO_3)_2$ (H_2L = μ_2-*N*′¹,*N*′²-di(isopropylidene)oxalohydrazide).[16] The present work is devoted to the synthesis, features of the structural organization of a new coordination polymer of silver(I) based on acetone oxalohydrazide dihydrazone, as well as the study of its thermal behavior and luminescent properties.

The coordination polymer $[Ag_2L]_n$ (**1**) was prepared from $AgNO_3$ by *in situ* condensation of oxalohydrazide with acetone (Scheme 1).



Scheme 1

The addition of aqueous ammonia ensured complete deprotonation of H_2L to L^{2-}, facilitating the formation of the polymer structure.

© Mendeleev Communications.

According to IR spectroscopy (

Figure S1), the absence of ν(N–H) bands in the region of 3370–3270 cm^{-1} confirms ligand deprotonation. The band at 1662 cm^{-1} is assigned to ν(C=O), which is consistent with literature data for related hydrazide complexes. The bands at 1581 and 1504 cm^{-1} are assigned to ν(C=N), the bands at 1246 and 1107 cm^{-1} to ν(C–N)/ν(N–N).[17–19] The weak bands at 2083, 1994, and 1917 cm^{-1} are characteristic of solvate CH_3CN; the broad band at 3224 cm^{-1} is for H_2O. The absence of the nitrate band (~1384 cm^{-1}) confirms the neutral nature of complex **1**.[20]

According to X-ray data, compound **1** crystallizes in the trigonal space group *R*-3 and is a 3-D coordination polymer with solvent-accessible channels (Figure 1), formed by coordination interactions of silver ions with all six heteroatoms of the organic ligand (four nitrogen atoms and two carbonyl oxygen atoms). The ligand adopts a transoid conformation and occupies a special position in the crystal on an inversion center located in the midpoint of the C–C single bond. In the polymer structure, the ligand is bound to four silver ions, forming a system of fused five-membered N,O-chelate metallocycles. The chelate rings are pairwise non-equivalent. One chelate ring is formed by coordination of the carbonyl oxygen atom and the deprotonated amide nitrogen N(1) and is planar, with the silver ion deviating from the NCCO plane by 0.35 Å. The second chelate ring is formed by coordination through the same carbonyl oxygen and the azomethine nitrogen atom N(2) and adopts an envelope conformation, with the silver ion deviating from the NNCO plane by 1.33 Å. Each silver ion in the polymer structure is bound to two nitrogen atoms N(1) and N(2) from two adjacent ligands with slightly different Ag–N distances of 2.198(2) and 2.179(2) Å; the N–Ag–N angle of 155.71(8)° deviates significantly from linearity. Additionally, due to weaker secondary interactions, the silver ion is bound to two carbonyl oxygen atoms with significantly increased Ag–O distances of 2.418(2) and 2.606(2) Å and an O–Ag–O angle of 120.64(8)°, completing its coordination environment to CN_{Ag} = 4 (τ_4 = 0.54). It is noteworthy that examples of simultaneous coordination of all potential N,O-donor atoms of hydrazide-hydrazone ligands to metal ions are few.[21–23] In most known cases, such ligands bind only partially – via one nitrogen atom, only oxygen centers, or two nitrogen atoms, and full chelate coordination is often achieved with the participation of alkali metal cations.[24] In the presented structure, by contrast, the ligand coordinates to four silver ions via all available heteroatoms without the involvement of additional metal centers.

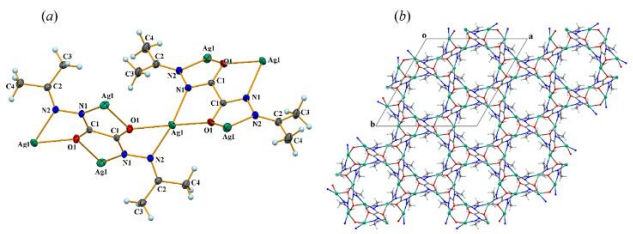


Figure 1 (*a*) A fragment of polymeric structure **1** depicting the atomic numbering scheme and the coordination environment of the silver ion (thermal ellipsoids are drawn at the 50% probability level); (*b*) crystal packing diagram for **1** (projection along c axis).

In the crystal, coordination polymer **1** forms a honeycomb structure with channels along the -3 inversion axis. These hexagonal voids have considerable dimensions: the distance between opposite silver ions in the channel walls is 9.337(1) Å, and between the nearest hydrogen atoms of methyl groups is 4.9 Å. They are filled with highly disordered acetonitrile/water solvent molecules in a 1:3 ratio, which do not form strong intermolecular contacts with the metal–organic framework.

The thermal behavior of **1** was studied by the method of simultaneous thermal analysis (STA) in an argon atmosphere with simultaneous recording of mass loss (TG) curves and thermal effects (DSC) (for details, see Online Supplementary Materials Figure S2).

Thermolysis occurs in several stages. The first, weakly expressed (54–60 °C), corresponds to the removal of residual solvate molecules on the mass loss curve (TG, Figure S2, *A*) (m_{calc} / m_{found} = 3.7% / 3.2%). On the DSC curve, this process is accompanied by a weak endoeffect with an extremum at 56 °C (Figure S2, *B*).

The absence of hydrogen and other intermolecular interactions between the solvate molecules and the metal-organic framework results in such low dehydration values (although some hydrate molecules are lost during the sample drying stage). This is followed by a prolonged stage (65–275 °C), in which the simultaneous processes of desorption of acetonitrile solvate molecules and chemical transformations of gaseous products characteristic of the thermal decomposition of hydrazones, accompanied by the rupture of C–N, C–C and N–N bonds and the release of gaseous products (NH_3, N_2H_4, CO, CO_2, etc.) occur.[18,19,25] The DSC curve shows a strong exothermic effect with an extremum at 245 °C, which is in good agreement with the decomposition temperature of free oxalohydrazide (242–244 °C).[17] A similar thermolysis pattern was observed for the previously studied silver complex $[\{Ag_7(nfur)_8\}\{Ag(CH_3CN)_2\}]_n$[26] – the process was also characterized by the formation of various N-containing products. The final stage (275–500 °C) is greatly extended over the temperature range; here, the final thermal destruction processes occur, and the final mass corresponds to pure silver (m_{calc} / m_{found} = 52.4% / 33.2%). The observed mass loss following thermolysis can be attributed to the volatility of the final product. Although this is not characteristic of silver, reports in the literature do note the volatility of the final compounds of certain *d*-block metals (such as zinc sulfide[27]), including silver[28,29]. The results of electron microscopy and EDX data (Figure S2, *C, D*) indicate the formation of silver nanoparticles after thermolysis.

The excitation and emission spectra of compound **1** (Figure 2) were recorded for a solid powder sample at room temperature. The excitation spectra at λ_{em} = 425 nm contain strong bands at 232 and 260 nm with shoulders at 251, 272, and 300 nm, which corresponds to π→π* and n→π* intramolecular transitions in the conjugated system of the hydrazone (C=N, C=O, N–N bonds). The emission spectrum at λ_{ex} = 260 nm consist of broad bands with maxima at 427, 490 and 536 nm and is related to ligand-centered fluorescence (IL).[30,31]

© Mendeleev Communications.

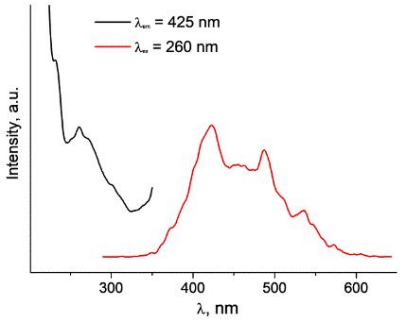


Figure 2 Solid-state excitation and emission spectra of **1**.

Thus, in the presence of aqueous ammonia, the reaction of silver nitrate with acetone oxalohydrazide dihydrazone leads to complete deprotonation of the ligand and the assembly of a three-dimensional coordination polymer with hexagonal channels (occupied by solvent molecules) measuring ~9.3 × 4.9 Å. A distinctive feature of the crystal architecture of **1** is the combination of the chelating and bridging functions of L^{2-}, forming pairwise nonequivalent metallocycles, reflecting the high adaptability of the Ag^{+} coordination sphere. Thermolysis of the compound occurs in multistage steps, forming silver nanoparticles at relatively low temperatures (up to 500 °C), opening up prospects for its use as a precursor for the production of metallic nanomaterials.

This research was funded by the Russian Science Foundation (project No. 25-23-00469). We are grateful to the User Facilities Center of Institute of General and Inorganic Chemistry of the Russian Academy of Sciences for physicochemical measurements.

Crystallography in the Manuscript. Details of the data collection are given in a footnote.[=]

Online Supplementary Materials

Supplementary data associated with this article can be found in the online version at doi:

References

1 A. Ullah, N. U. Islam, M. Ali, M. Ahmad, H. Ullah, K. Aziz, I. Shakir, M. Z. Azam, S. Mukherjee, N. V. Minh and Y. Xie, *Rev. Inorg. Chem.*, 2026; https://doi.org/10.1515/revic-2026-0018.
2 A. G. Young and L. R. Hanton, *Coord. Chem. Rev.*, 2008, **252**, 1346; https://doi.org/10.1016/j.ccr.2007.07.017.
3 C. E. Housecroft, *Coord. Chem. Rev.*, 1994, **131**, 1; https://doi.org/10.1016/0010-8545(94)80090-1.
4 M. A. Carvajal, J. J. Novoa and S. Alvarez, *J. Am. Chem. Soc.*, 2004, **126**, 1465; https://doi.org/10.1021/ja038416a.
5 E. M. Njogu, B. Omondi and V. O. Nyamori, *J. Coord. Chem.*, 2015, **68**, 3389; https://doi.org/10.1080/00958972.2015.1070147.
6 D. S. Yambulatov, I. A. Lutsenko, D. E. Baravikov, F. M. Dolgushin, T. V. Astaf'eva, O. B. Bekker, L. G. Nersisyan, M. A. Samvelyan, T. V. Ghochikyan, M. A. Kiskin, I. L. Eremenko and V. K. Ivanov, *Molecules*, 2023, **29**, 105; https://doi.org/10.3390/molecules29010105.
7 T. Elkoush, N. D. Reich and M. G. Campbell, *Angew. Chem.*, 2021, **133**, 22794; https://doi.org/10.1002/ange.202106937.
8 L. R. V. Favarin, L. B. Oliveira, H. Silva, A. C. Micheletti, L. Pizzuti, A. Machulek-Júnior, A. R. L. Caires, D. F. Back, S. M. Lima, L. H. C. Andrade, L. F. B. Duarte, L. M. C. Pinto and G. Antônio Casagrande, *Inorganica Chim. Acta*, 2019, **492**, 235; https://doi.org/10.1016/j.ica.2019.04.043.
9 M. Harmata (ed.), *Silver in Organic Chemistry*, 1st ed., Wiley, Hoboken, 2010; https://doi.org/10.1002/9780470597521.
10 S. Medici, M. Peana, G. Crisponi, V. M. Nurchi, J. I. Lachowicz, M. Remelli and M. A. Zoroddu, *Coord. Chem. Rev.*, 2016, **327–328**, 349; https://doi.org/10.1016/j.ccr.2016.05.015.
11 C. Seward, J. Chan, D. Song and S. Wang, *Inorg. Chem.*, 2003, **42**, 1112; https://doi.org/10.1021/ic020480q.
12 K. Elankathirselvan, K. Srinivasan, S. Parveen and W. T. A. Harrison, *J. Mol. Struct.*, 2025, **1324**, 140925; https://doi.org/10.1016/j.molstruc.2024.140925.
13 L. V. Tamayo, A. F. Santos, I. P. Ferreira, V. G. Santos, M. T. P. Lopes and H. Beraldo, *BioMetals*, 2017, **30**, 379–392; https://doi.org/10.1007/s10534-017-0013-2.
14 H. Kargar, M. Fallah-Mehrjardi and K. S. Munawar, *Coord. Chem. Rev.*, 2024, **501**, 215587; https://doi.org/10.1016/j.ccr.2023.215587.
15 E. Costa-Villén, M. Ortiz, P. Sitjar, C. Puigjaner and M. S. El Fallah, *Magnetochemistry*, 2025, **11**, 4; https://doi.org/10.3390/magnetochemistry11010004.
16 R. Nimthong, N. Thepsena, W. Puetpaiboon and Y. Wattanakanjana, *Acta Crystallogr. Sect. E Struct. Rep. Online*, 2014, **70**, m30; https://doi.org/10.1107/S1600536813034454.
17 S. P. Perlepes, F. J. Quaeyhaegens and H. O. Desseyn, *Transit. Met. Chem.*, 1990, **15**, 132; https://doi.org/10.1007/BF01023902.
18 K. A. Melha, *J. Enzyme Inhib. Med. Chem.*, 2008, **23**, 285; https://doi.org/10.1080/14756360701448073.
19 D. Z. Obadovic, D. M. Petrovic, V. M. Leovac and S. Caric, *J. Therm. Anal.*, 1990, **36**, 99; https://doi.org/10.1007/BF01912072.
20 A. F. Santos, I. P. Ferreira, C. B. Pinheiro, V. G. Santos, M. T. P. Lopes, L. R. Teixeira, W. R. Rocha, G. L. S. Rodrigues and H. Beraldo, *ACS Omega*, 2018, **3**, 7027; https://doi.org/10.1021/acsomega.8b00533.
21 M. Sutradhar, E. C. B. A. Alegria, T. R. Barman, M. F. C. Guedes Da Silva, C.-M. Liu and A. J. L. Pombeiro, *Front. Chem.*, 2020, **8**, 157; https://doi.org/10.3389/fchem.2020.00157.
22 D. Liu, Z. Chen, W. Huang, S. Qin, L. Jiang, S. Zhou and F. Liang, *Inorganica Chim. Acta*, 2013, **400**, 179; https://doi.org/10.1016/j.ica.2013.01.035.
23 S.-X. Huang, F. Xu, S.-J. Qi, K. Wang, Y. Li, S.-H. Zhang, X.-Q. Zhang, S.-Y. Luo and F.-P. Liang, *J. Clust. Sci.*, 2021, **32**, 765; https://doi.org/10.1007/s10876-020-01838-z.
24 S. Gupta, M. V. Kirillova, M. F. C. Guedes Da Silva, A. J. L. Pombeiro and A. M. Kirillov, *Inorg. Chem.*, 2013, **52**, 8601; https://doi.org/10.1021/ic400743h.
25 V. V. Rodè, E. M. Bondarenko, V. V. Korshak, A. L. Rusanov, E. S. Krongauz, D. A. Bochvar and I. V. Stankevich, *J. Polym. Sci., Part A: Gen. Pap.*, 1968, **6**, 1351; https://doi.org/10.1002/pol.1968.150060526.
26 K. A. Koshenskova, L. S. Razvorotneva, F. M. Dolgushin, O. B. Bekker, A. V. Kuchin, L. L. Frolova, A. S. Zaeva, T. N. Pozmogova, M. A. Shestopalov, V. I. Komlyagina, A. L. Gushchin, I. L. Eremenko and I. A. Lutsenko, *Inorg. Chem. Commun.*, 2026, **191**, 116989; https://doi.org/10.1016/j.inoche.2026.116989.
27 A. V. Ivanov, I. A. Lutsenko, A. S. Zaeva, A. V. Gerasimenko, E. B. Merkulov, S. A. Leskova, *Russ. J. Coord. Chem.*, 2007, **33**, 815; https://doi.org/10.1134/S107032840711005X.
28 J. Jurczyk, C. Glessi, K. Madajska, L. Berger, J.I.K. Nyrud, I. Szymańska, C. Kapusta, M. Tilset, I. Utke, *J. Therm. Anal. Calorim.*, 2022, **147**, 2187; https://doi.org/10.1007/s10973-021-10616-6.

[=] X-ray diffraction experiment was carried out with a Bruker SMART Photon-II CCD diffractometer (graphite monochromated Mo-Kα radiation, λ = 0.71073 Å). The structure of the compound obtained was solved by direct methods and refined in the full-matrix least-squares anisotropic approximation using the SHELXL[32] and Olex2[33]. Hydrogen atoms positions were calculated and were then refined in isotropic approximation within the riding model.
Crystal data for **1** (T = 100 K): $C_8H_{12}Ag_2N_4O_2 \cdot 0.167(C_2H_3N) \cdot 0.5(H_2O)$, M = 427.81, trigonal, $R\bar{3}$, $a = b$ = 20.3701(12), c = 8.3280(6) Å, V = 2992.7(4) Å^3, Z = 9, d_{calc} = 2.136 g/cm^3, μ = 2.943 mm^{-1}. Total of 11963 reflections were collected ($2\theta_{max}$ = 60°), from which 1934 were independent (R_{int} = 0.0453). The final refinement parameters were R_1 = 0.0261 for 1719 reflections with $I > 2\sigma(I)$, and wR_2 = 0.0612 for all reflections, GOOF = 1.096. Maximum and minimum of residual electronic density were 0.499 and -0.660 eÅ^{-3}.
CCDC 2570128 contains the supplementary crystallographic data for this paper. These data can be obtained free charge from the Cambridge Crystallographic Data Centre http://www.ccdc.cam.ac.uk

© Mendeleev Communications.

29 E. S. Vikulova, S. I. Dorovskikh, T. V. Basova, A. A. Zheravin, N. B. Morozova, *Molecules*, 2024, **29**, 5705; https://doi.org/10.3390/molecules29235705.
30 D. Ray, E. S. S. Iyer, K. K. Sadhu and P. K. Bharadwaj, *Dalton Trans.*, 2009, 5683; https://doi.org/10.1039/b820481k.
31 A. Kuznetsova, V. Matveevskaya, D. Pavlov, A. Yakunenkov and A. Potapov, *Materials*, 2020, **13**, 2699; https://doi.org/10.3390/ma13122699.
32 G. M. Sheldrick, *Acta Crystallogr. Sect. Found. Adv.*, 2015, **71**, 3; https://doi.org/10.1107/S2053273314026370.
33 O. V. Dolomanov, L. J. Bourhis, R. J. Gildea, J. A. K. Howard and H. Puschmann, *J. Appl. Crystallogr.*, 2009, **42**, 339; https://doi.org/10.1107/S0021889808042726.

Received: 7th August 2026; Com. 26/8170

© Mendeleev Communications.